

Universidade de Évora - Escola de Ciências e Tecnologia

Mestrado em Engenharia Mecatrónica

Dissertação

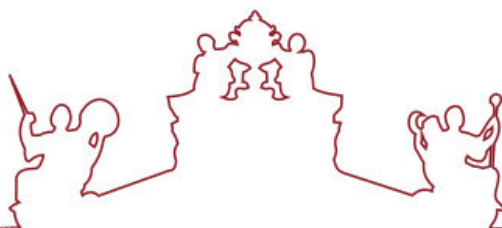
**Analysis and optimization of riveting processon relay's
components**

Tiago Alexandre Salvador Pereira

Orientador(es) | Pedro Areias

M. P. Dos Santos

Évora 2021



Universidade de Évora - Escola de Ciências e Tecnologia

Mestrado em Engenharia Mecatrónica

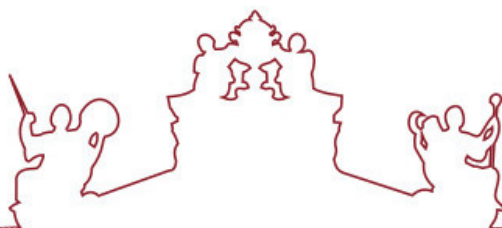
Dissertação

**Analysis and optimization of riveting processon relay's
components**

Tiago Alexandre Salvador Pereira

Orientador(es) | Pedro Areias
M. P. Dos Santos

Évora 2021



A dissertação foi objeto de apreciação e discussão pública pelo seguinte júri nomeado pelo Diretor da Escola de Ciências e Tecnologia:

Presidente | Fernando Manuel Janeiro (Universidade de Évora)

Vogais | Pedro Alexandre Rodrigues Carvalho Rosa (Instituto Superior Técnico)
(Arguente)
Pedro Areias (Universidade de Évora) (Orientador)

Contents

1	Introduction	7
2	Studied model and configuration	8
2.1	Geometry and kinematics	8
2.2	Boundary conditions	9
2.3	Riveting stages	10
2.3.1	Rivet elastic deformation	10
2.3.2	Rivet plastic deformation	12
3	Material modeling and properties	13
3.1	Punch	13
3.2	Terminal	14
3.3	Rivet	16
4	Explanation of mechanical equipment and brief consideration	18
5	Deformation, damage and material behaviour	20
5.1	Deformation	20
5.2	Damage	21
5.3	Material behaviour	22
6	Simulation and analysis	23
6.1	Meshing	23
6.1.1	Mesh type	23
6.1.2	Mesh refinement	25
6.2	Simulation results	28
6.3	Analysis and comparison of results	31
7	Electrostatics and full temperature coupling	34
8	Optimization	39
8.1	Optimal riveting	39
8.2	Punch deterioration	41
9	Conclusion	44
10	Acknowledgements	45

Análise e optimização do processo de cravamento em componentes de relés

Resumo

O processo de rebitagem é um dos métodos mais importantes para unir duas ou mais peças. O sucesso da fixação dessas peças dependerá de diferentes variáveis, como a geometria das peças envolvidas, os seus materiais, as restrições e a magnitude da carga exercida sobre o sistema. Neste estudo, tendo em consideração um problema industrial real, nomeadamente a deformação de um rebite numa única peça de forma a criar um contacto, um modelo numérico de elementos finitos foi desenvolvido com o auxílio do software ABAQUS, de forma a ser possível comparar os resultados obtidos da simulação com a realidade em termos de força e deformação plástica. A comparação desses resultados irá validar a abordagem e criar uma forma de otimizar este processo de forma a minimizar defeitos indesejáveis no material como por exemplo o fender do rebite devido a excesso de força ou deformação.

Analysis and optimization of riveting process on relay's components

Abstract

The riveting process is one of the most significant methods to join/fasten two or more parts. The success of fastening these parts will depend on different variables such as the geometry of the parts involved, its materials, constraints and the magnitude of the load exerted onto the system. In this study, taking into account a real industrial problem, which is the deformation of a rivet onto a single metal sheet in order to create a contact, a finite element numerical model is developed with the aid of the software ABAQUS, in a way to compare our results with the reality in terms of force and plastic deformation. The comparison of these results will validate our approach and create a form to optimize this process in order to minimize undesirable defects on the material such as the cracking of the rivet due to excess of force or over deformation.

1 Introduction

Riveting is a common process used on the industry, mainly with the single purpose of joining two or more structures together, such as metal sheets. Specifically, it is a widely used process in aeronautic and aerospace industries. However, in our process, the riveting will have another purpose beyond joining different parts or structures. We are dealing with a single metal sheet, and deform the rivet in such a way that it will fill the preexisting hole and will be tightly secure onto the metal sheet, hence ensuring a perfect electrical connection between these two different parts.

This type of mechanical connection will play a great role in establishing a perfect electrical connection, as it is a requirement to achieve the quality of the final product. In this particular electromechanical industry, some products such as relays, sensors and others, use riveted contacts to conduct electrical load through its terminals. Therefore, a less successfully riveting, may not only compromise the integrity of the whole joint, but its conductivity by increasing the electrical resistance, thus meddling with the performance of the final product.

Although there are many types and configurations of rivets, these may be particularly divided into six different groups. In this particular case, regarding the purpose of our riveting, as described above, we'll be considering the *button head* rivet.

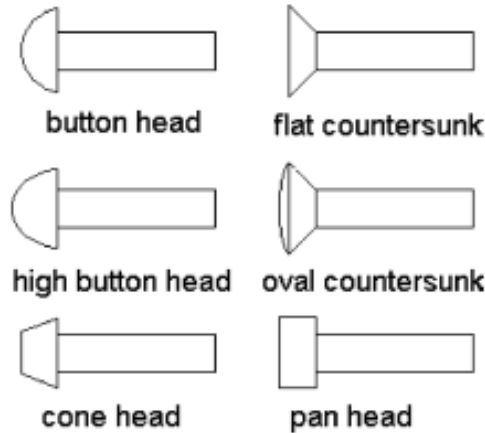


Figure 1: Distinct types of rivets. [10]

Hence, in order to allow for a simulation with the aim to attain some pertinent data, such as the stress, strain and plastic deformation of the riveted joint, and therefore to compare it with the results from the process itself, the mechanical model of this process will be built and analyzed, with the aid of a finite element method (FEM) software. Furthermore, afterwards a valid riveting simulation is achieved, the behavior of that joint when passing an electrical load, which after all, is its main purpose, will also be replicated, so an explicit and rigorous analysis of the true effectiveness of the riveting is accomplished.

2 Studied model and configuration

2.1 Geometry and kinematics

The geometry of the studied model is quite simple. As mentioned, there is only one sheet of metal, which is the terminal, one rivet, that will be deformed to form the contact, from which an electrical current will be conducted and a punch, that will be used to deform the rivet shank, punch which will be moving vertically along the Y axis (fig. 2).

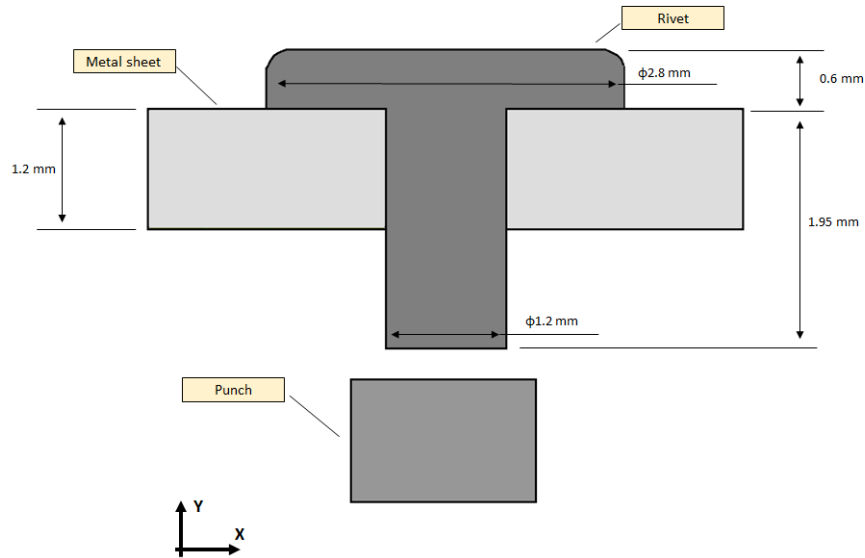


Figure 2: Model under study.



Figure 3: Actual picture of the components to joint.

2.2 Boundary conditions

The real conditions to which riveted joint are submitted while being worked on the actual machine are reproduced. To that purpose, some constraints have to be defined. Although on the process itself we'll have a counter-punch or upper die limiting the movement of the rivet head, here to simplify matters, we'll assume that the rivet head is fixed along all axis, X, Y and Z.

The terminal or metal sheet is also constrained on all of its degrees of freedom. Considering that it will be hold tight on the machine during the riveting process, hence theoretically not being able to move on any direction, in the simulation will be defined as having its edges as clamped.

Lastly the punch, will also be constrained along Y and Z axis direction, however it will have displacement along X, recreating the movement of the punch towards the rivet shank, causing then the elasto-plastic deformation of the rivet. These boundary conditions defined are depicted on figure 4.

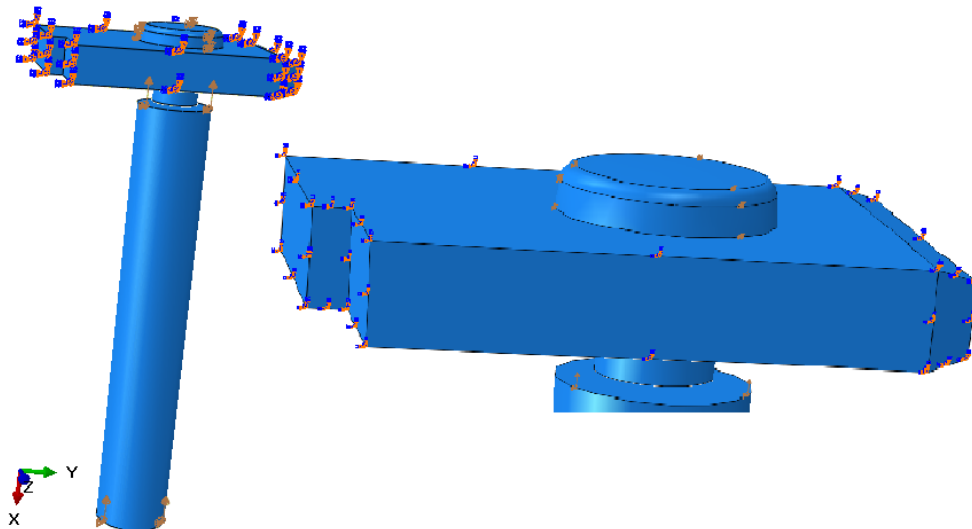


Figure 4: Boundary conditions.

2.3 Riveting stages

This riveting process that we have depicted here, like most of the known riveting processes, may be characterized into two different main stages, where the rivet will behave differently whilst is being compressed. These two different stages are:

1. Rivet elastic deformation;
2. Rivet plastic deformation;

Table 1: Riveting stage variables

Quantity	Description	Units
σ_x	Stress on x direction	Pa
F	Load	N
S	circular section	mm^2
d_1	initial diamter	mm
d_2	final diameter	mm
l_1	initial length	mm
l_2	final length	mm
ϵ	Strain	-
E	Young's modulus	Pa
x	punch displacement	mm

2.3.1 Rivet elastic deformation

This initial stage correspond to the moment the punch first have contact with the rivet shank and till the moment that we'll start to have plastic deformation. At this stage, the force needed to keep deforming the rivet shank will increase proportionally to the displacement of the punch, since the elastic deformation goes according to Hooke's law. Hence, the stress on the rivet shank, along the x direction, will be given by

$$\sigma_x = \frac{F}{S} = \frac{4F}{\pi d_1^2} \quad (1)$$

where F is the force applied upon the rivet shank, S the circular section of rivet shank and d the diameter of that section.

Moreover, the strain along this direction may also be defined as

$$\epsilon_x = \frac{l_2 - l_1}{l_1} = \frac{\Delta l_{elast}}{l_1} \quad (2)$$

or, using Hooke's law, as

$$\epsilon_x = \frac{\sigma_x}{E} = \frac{4F}{E\pi d_1^2} \quad (3)$$

where E is Young's modulus, l_1 the initial length of the rivet shank and l_2 the final length, therefore the elastic deformation of the rivet along this axis may expressed as

$$\Delta l_{elast} = \frac{4Fl_1}{E\pi d_1^2} \quad (4)$$

2.3.2 Rivet plastic deformation

The plastic deformation stage occurs when the rivet reaches its yield stress limit, thus from this point on, all the deformation imposed by the punch will permanently deform the rivet. At this point, unlike the previous stage where Hooke's law illustrate the rivet behavior, here it will be correlated with the elasto-plastic behavior of the material.

Throughout this process, we'll have the rivet shank starting to deform in a way that it will start to make contact with the interior on the metal sheet preexisting hole as it will also start to flatten the tip of the shank, in a way that it will start to make contact with the back part of the metal sheet, thus acting like a plug and therefore assuring a proper fixation, just like represented on figure 5.

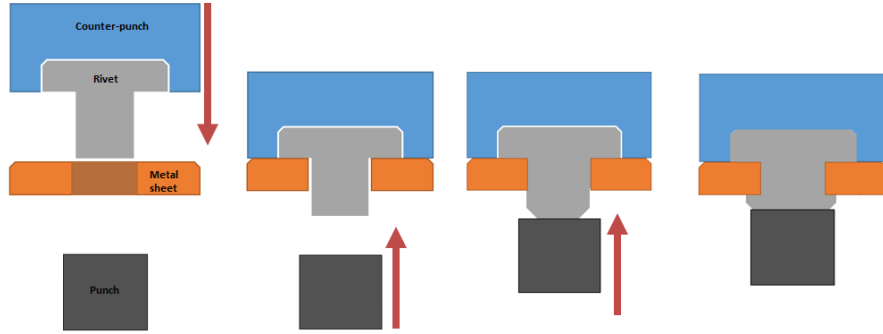


Figure 5: Rivet shank diameter schematic before, during and after riveting

So that the new diameter of the rivet shank may be expressed as

$$d_2 = d_1 + \Delta d_1 \quad (5)$$

As previously seen, at this point, the stress at the rivet shank along x axis may be expressed as

$$\sigma_{plastx} = \frac{F_{plast}}{S_{plast}} = \frac{4F_{plast}}{\pi d_2^2} = \frac{4F_{plast}}{\pi(d_1 + \Delta d_1)^2} \quad (6)$$

Furthermore, considering x the displacement of the punch, the full plastic deformation of the rivet shank may be expressed as

$$\Delta_{plast} = x - abs(\Delta l_{elast}) = x - \frac{4Fl_1}{E\pi d_1^2} \quad (7)$$

3 Material modeling and properties

In order to become possible to simulate and to analyze this riveting process, the material properties for these parts and tools involved, specifically terminal, rivet and punch needs to be defined. Most of these, namely terminal and punch are homogeneous, thus expected to have an isotropic behaviour since are made with the same material, however this won't be exactly the case for the rivet.

3.1 Punch

The punch throughout this whole process will be only a tool with the purpose to impose a deformation upon the riven shank, hence fastening it upon the metal sheet. Its material, HSS, is known due to the fact that's what is stated in its official drawing, therefore, for this item, typical steel values were used to define it. Worth mentioning that since this will be only a tool to be used to simulate the riveting (fig. 6), there's no much interest on its own behaviour and deformation, therefore its plastic behavior was not defined.

Table 2: Mechanical properties of the punch

Mechanical properties	Punch
Mass density	8138 [kg/m ³]
Young's modulus	210 [GPa]
Poisson coefficient	0.30

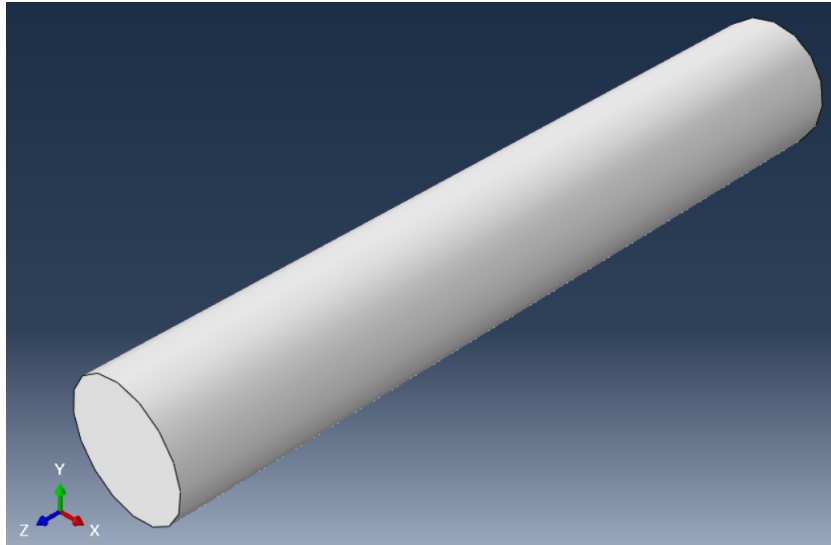


Figure 6: Punch used on simulation - geometry identical to the one used in the process

3.2 Terminal

The terminal, represented on figure 7, which in this specific situation is the sole metal sheet to be riveted, like the punch above, is from a known material, which in accordance with its drawing, will be copper with a pre-tinned coat, hence for the purpose of assessing its elasto-plastic behaviour when being compressed during riveting, it will be treated as copper.

Table 3: Mechanical properties for the terminal

Mechanical properties	Terminal
Mass density	8960 [kg/m ³]
Young's modulus	130 [GPa]
Poisson coefficient	0.34

Yet, unlike section 3.1, plasticity is quite relevant for this item, since this one will be a part of the riveted joint, therefore in order to obtain these values for the characteristic Stress and Strain, we used the data for high purity copper from its Stress-Strain graphic at room temperature (300 K) from “*Tensile Deformation Of High-purity Copper As A Function Of Temperature, Strain Rate And Grain Size*” from R. P. Carreker, Jr. and W. R. Hibbard, Jr [3]. With that, and resorting to *Get Data Graph Digitizer* software, it became possible to withdraw the data presented on table 4.

Table 4: Hardening curve for the terminal

Yield Stress	Plastic Strain
70826644.235	0
97808222.991	0.0114907795761
120453476.590	0.0223036085292
141653288.469	0.0356756742238
161407658.630	0.0500695006829
179234773.165	0.0636902915268
195616445.981	0.0780765971391
213925374.423	0.0947734143436
229825233.333	0.112746089495
242834208.805	0.128918596234
257770439.902	0.149195336538
268370345.842	0.168949915189
279933879.594	0.189987872634
291015599.440	0.211793493662
301615505.381	0.235391762255
309324527.882	0.254627402474
317515364.290	0.272582887119

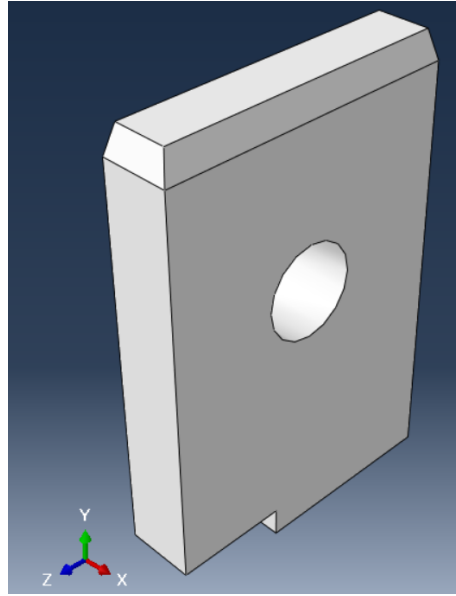


Figure 7: Terminal used on simulation - geometry identical to the one used in the process.

3.3 Rivet

The rivet (fig. 9) will be maybe the most important part at all of this process, since it's the one that not only has to be fixed to the metal sheet, but also has to ensure a proper path for an electrical load, therefore it will be the utmost importance to correctly define its material properties.

As it may be seen below by the picture from the actual rivet, this part is not at all a solid piece composed by the same material. The bottom part is made from electrolytic copper, which is basically high purity copper that was attained through a purification by electrolysis, whilst the top part of the rivet, the actual part that will serve as an actual contact, is made from $AgSnO_2$, which is a silver tin oxide, material which is produced by a powder sintering process and widely used on the electromechanical industry due to its good power switching characteristics, however, we still do not have some precise knowledge about this material, in particular, about its plastic behaviour. Thus, in a way to contour this problem, several of these specimens were tested at *INEGI* institute, using a displacement control method of 0.2 mm/min and a load stiffness obtained by testing of 2817.93 N/mm. For each of these specimens, a preload of 25N was applied and this test was performed in a way to cease at the maximum displacement of 1mm.

Hence, with this assessment of the mechanical properties of these rivets, we could reach its Stress-Strain characteristic curves, which may be seen depicted on picture 8, and with them, the much needed data for definition of the plastic behaviour of this part could be withdrawal.

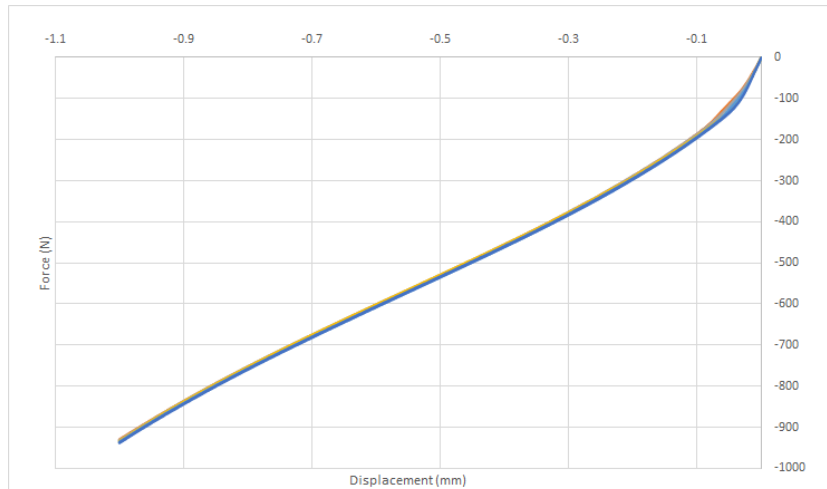


Figure 8: Rivet force-displacement curves

Now, in possession of these characteristics curves and the data used to plot them, inputs which were kindly provided by *INEGI*, we're finally in conditions to characterize these rivets plastic behaviour, characterization which may be observe at table 5.

Table 5: Hardening curve for the rivet

Yield Stress	Plastic Strain
5347647.035	0
40855079.749	0.010116115102392
114725825.977	0.05076337082051
197614448.669	0.100524777938074
223157444.251	0.2015486261523
255285865.343	0.301390374896355
288773570.456	0.503678383268768
298876217.166	0.664459771736317

Concerning the remaining mechanical characteristics needed to be defined, the same mechanical properties of copper, as used on point 3.2. were applied, considering the fact that this part is mainly copper.

Table 6: Mechanical properties for rivet

Mechanical properties	Terminal
Mass density	8960 [kg/m ³]
Young's modulus	130 [GPa]
Poisson coefficient	0.34

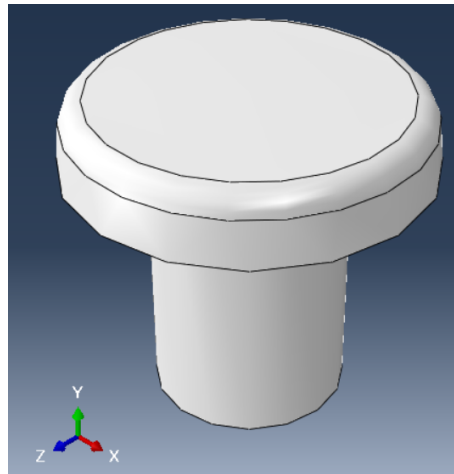


Figure 9: Rivet used on simulation - geometry identical to the one used in the process

4 Explanation of mechanical equipment and brief consideration

In order to provide some insight into the process where this riveting occurs, the mechanics of this particular machine is going to be briefly detailed. First and foremost, the machine had to be instrumented with a load cell, in order to measure the magnitude of load exerted during the riveting and with a displacement sensor, so it could be correlated the force measured with the moment where it occurs. Without both of these process outputs that are related to one another, a thorough and live analysis of the process couldn't be attained, though we had to settle only for the monitoring of the output of the product and not the process.

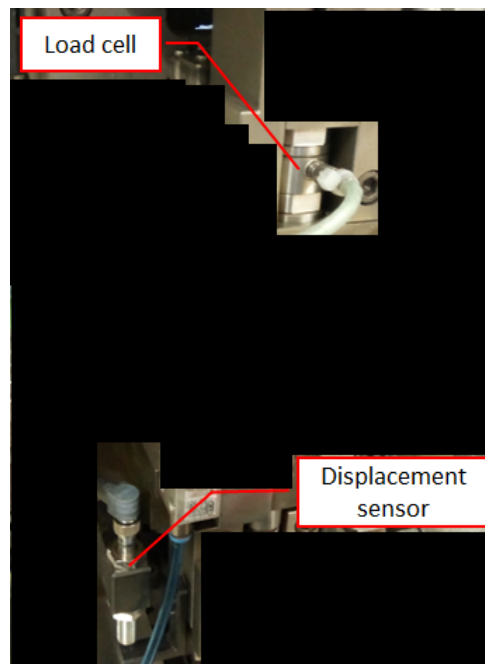


Figure 10: Machine overall

The riveting here in this process, basically occurs in three different step, where the terminal is put into position, the lowering and holding of the rivet through the terminal pre-existent hole and the advance of the punch with the aim to deform the rivet shank.

In this process, it's the same tool that pick up the rivet and inserts it throughout the terminal. This tool will also act like a counter-punch since it is designed to restrain any movement of the rivet's head and therefore to support it during the action of the punch that deforms the rivet shank, hence the reason why on section 2.2, *Boundary Conditions*, it was assumed that the rivet's head would be constrained along all its degrees of freedom.

Moreover, it is relevant to note that in this situation, the load cell is attached to the tool that presses the counter-punch, therefore the data from the experimental/real tests are actually the reaction force obtained through the riveting, so as obvious, a poor contact between rivet head and

counter-punch will not only contributes for a improper riveting, but it will also provides a deceitful measurement.

Regarding the punch, it is embedded on a different tool, a punch holder, tool which maintains the punch always fully hidden when idle, and only when on its working position will it allows the punch tip to overhangs and therefore deform the rivet shank. Thus, the way this mechanism is designed, excepting for vertically, it will contain the movement of punch on all the other remaining axis, so all the displacement traveled by this punch will necessarily be made towards the rivet shank.

5 Deformation, damage and material behaviour

In a way to better understand and to have a similar result attained from the FEM simulation when comparing it to the experimental results, it is important to have the correct equations and model approach so the results may be the closest as possible to the reality, otherwise, an inadequate model approach will provide wrong and unreliable results.

Moreover it is also pertinent to have some knowledge about the different kinds of materials, on how to characterize them and understand how are they expected to behave under certain conditions and how and why failures may occur.

5.1 Deformation

Mainly, materials may be roughly characterized as the following groups: rigid, elastic, plastic and viscoplastic.

Rigid

A rigid material or object is defined as a body that the distance between to given points is always the same, regardless of the force applied, meaning that this particular body would never deform or change in any way its geometry under any circumstances. Meaning that in fact, such thing does not occur in reality, hence this consideration merely exists to simplify the understanding of certain circumstances.

Elastic

An elastic material may be characterized as a material than when stress is applied, it will be possible to observe a deformation on its geometry, deformation which is reversible when the previous stress applied is unload, hence it is fair to state that the strain on an elastic object is related to the stress applied, on an linear relation, thus behaving according Hook's law (fig. 11).

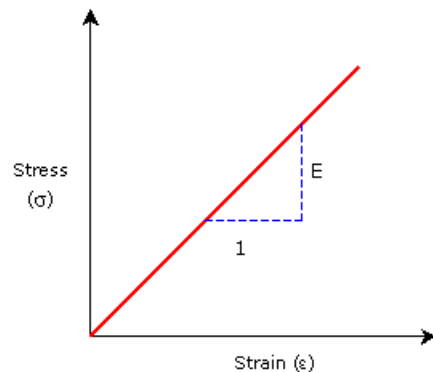


Figure 11: Elastic material Stress-Strain diagram

Plastic

By plastic objects it is meant that in this case, unlike the elastic materials, when the stress previously applied that caused a deformation is unloaded, we won't have a regression of the object's geometry to its original state, therefore this means that plastic solids are characterized by having a permanent strain, even though there's no longer load applied.

Moreover, into this plastic characterization of materials, we may also describe those as rigid-plastic solids and elasto-plastic solids. On the first one, a rigid-plastic solid is an object which will only deform when the load applied surpasses the yields stress, and when such happens, the object will deform evenly at the same rate when under the same constant load. On other hand, an elasto-plastic solid when subjected to a load which its magnitude is lower than the yield stress, will deform linearly, much like an elastic object, however, when its load surpass the yield stress, will then deform evenly at constant stress.

Viscoplastic

Viscoplasticity describes the inelastic behaviour of objects which its deformation will depend on the rate that loads are applied to it, therefore this is a rate dependent plastic deformation phenomenon, which like the plastic deformations described above, objects will be permanently deformed, but in this case, the deformation is related to the strain rate, where higher rates will increase the stress flow.

5.2 Damage

As seen above, materials may have in a simplistic way, elastic and plastic deformations. Both of these cases are related on a micro-scale, to the movement of the atomic layers that constitute the materials. On an elastic deformation, atoms move but the distance between those will not change much, hence preserving the chemical bonds between them, thus this atomic displacement is reversible. On other hand, on plastic deformations, the displacement between atoms will be higher, so these will have to rearrange themselves in a way to withstand such displacements, thus this process becomes irreversible.

During the atomic displacements and rearrangements, micro-defects and imperfections will be created. These imperfections will undermine the behaviour of the material, since when these atomic displacement movements reach these critical points, the process of plastic deformation will no longer become possible to endure, hence there will be no other option than for the atomic bonds to break, therefore causing cracks on the object.

These damages may be characterized as *brittle*, when failure occurs only after a small strain, *ductile* when failure occurs at the plastic regime of the material, hence after a considerable strain is endured, *creep* when failure is time and thermally dependent, since this last one will accelerate the process of catastrophic failure, and *cycle fatigue* failure, when the material is subjected to a cyclic load, which will also locally increase the material temperature, and therefore bringing another important factor than may undermine the material wellbeing and contribute to the occurrence of fractures.

5.3 Material behaviour

As previously mentioned above on the beginning of this chapter, it is quite important to adopt a model approach to aid on the simulation of the expected material behaviour, especially when simulating an interaction between several metallic components, such is our situation with the riveting process. Specifically on our case, with the aid of Finite Elements software, such as ABAQUS, will be using the Johnson-Cook material model to help to predict the behaviour of our objects.

Johnson-Cook material model is a plasticity model widely used and quite suitable for high strain rate deformations of several materials, especially on metals. Its constitutive equation is empirical and provides the possibility to take into account the effects of stress-strain behaviour, strain rate and temperature, and therefore relate it with the equivalent stress.

So, the Johnson-Cook constitutive equation may be expressed as

$$\sigma_{eq} = [A + B\varepsilon_p^n] \cdot \left[1 + C \ln \left(\frac{\dot{\varepsilon}_p}{\dot{\varepsilon}_0}\right)\right] \cdot \left[1 - \left(\frac{T - T_{room}}{T_{melt} - T_{room}}\right)^m\right] \quad (8)$$

where A is the initial yield stress, B is a strain hardening parameter, n is a strain hardening exponent, C a strain rate sensitivity parameter and m is the temperature exponent, so, all of these are material constants. Furthermore, there's also ε_p which is plastic strain, $\dot{\varepsilon}_p$ and $\dot{\varepsilon}_0$ that represent plastic strain rate and reference strain rate, respectively. Finally there's T , T_{room} and T_{melt} that respectively stand for working temperature, room temperature and melting temperature.

Hence, looking closely to equation (8), we may divide this into 3 different parts, where the first term is related to the hardening law or the elasto-plastic behaviour, the second term accounts for the strain rate and the third and last term of this equation is related to the thermal effect. Additionally, it is relevant to also understand the Johnson-Cook failure model, which will account for the material damage, that may be written as

$$\varepsilon_f = [D_1 + D_2 e^{(D_3 \cdot \sigma^*)}] \cdot [1 + D_4 \ln(\dot{\varepsilon}_p)] \cdot \left[1 + D_5 \left(\frac{T - T_{room}}{T_{melt} - T_{room}}\right)\right] \quad (9)$$

where ε_f is the failure strain, D_1 to D_5 are material constants empirically obtained and σ^* is the triaxiality stress ratio. So, on this equation, we'll have expressed on its first term the stress triaxiality, on the second term the strain rate and on the third, the temperature influence.

6 Simulation and analysis

So, accordingly with the facts and details described above, the simulation of the riveting process using ABAQUS finite elements software was performed, so the results attained from the simulation could be compared with the real ones, in order to assess the effectiveness of our model .

6.1 Meshing

Before starting the analysis and simulation of our problem, we must first take into account a very import detail that directly affect exactness of the outcome of this simulation, which is the Meshing.

Although we may have an accurate design of the different parts to be worked on, since with a finite element software we are able to have CAD capabilities and therefore arrange a proper model that represents our problem, and also have the material characteristics of these different parts correctly defined, these may not be quite enough, since when using a FEA like we did, one must also consider what kind of mesh is going to use.

Our problem, like so many other, due to its complexity and due to all the different interactions that are going to exist between all these different parts, would be impossible to solve it as it is. Hence, the necessity to divide it into smaller portions arise, thus the meshing.

On a mesh, these smaller portions are usually called as domains, and these may be represented in almost any form, depending on the geometrical complexity of our elements. For each of every domain represented, a differential equation is going to be solved, resulting in an individual solution for these, solutions that when combined will form a final result of the whole model. Consequently, it is expected that smaller and more refined meshing are preferred, since these in theory will grant more accurate results, however this comes with a cost, which will turn the computation heavier and a solution for the system under analysis may take several days to achieve, which in particular was our case.

6.1.1 Mesh type

Commonly, scientific literature tend to classify the mesh types as one of two: Structured or Unstructured. On our particular problem, throughout trial and error method, we found the necessity to arrange our mesh, since some parts, like the rivet, due to a more complex geometric, couldn't properly worked out as it was.

Structured mesh

A Structured mesh (fig. 12) is easily identified for the regular shape of its grid, as normally displaying a rectangular or hexahedral grid, if in a 2D or 3D situation. In the standpoint of programming, this model is quite space efficient, since the neighbor relations are defined by store arrangement, meaning that these each of these domains that form the structure of the mesh may be enumerated in a way that neighboring queries are analytically made upon these elements.

Summarily, with a structured mesh:

- Preferable for simple geometries;
- Good accuracy of results;
- Lower speed of mesh generation;
- Different types of meshing that may be useful:
 - Hybrid: for incompressibility;
 - Incompatible mode: good for flexion problems
 - Reduced integration: lighter solution, but less accurate

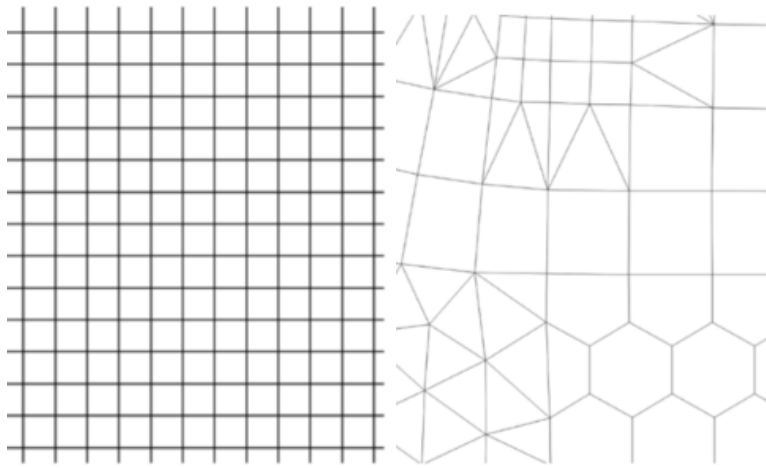


Figure 12: Structured and Unstructured mesh with different element types [21]

Unstructured

Similar to structured, unstructured mesh (fig. 12) can also be easily identified by the look of its irregular grid. These shapes may assume pretty much any geometry, although these are normally depicted as triangles or tetrahedral geometries, depending if in a 2D or 3D situation. Thus, solving problems with a more complex geometry that would be unattainable with the previous structured mesh, are now possible with this approach, since due to its wide range of different possibilities for geometrical domains and also by allowing different domains with different shapes to coexist, hence becoming possible to achieve a better fitting on all over the element.

Thus, summarily with an unstructured mesh:

- Good for complex geometries;
- Simple and sturdier;
- Good speed of mesh generation;
- Lower accuracy of results than structured meshes;

6.1.2 Mesh refinement

As discussed above on the previous section, the truthfulness of our results are directly connected to the quality of the mesh that is used to divide the whole system into smaller partitions. These partitions the smaller they get, so, the more refined and finer they are, the more a solution will become closer to the reality. This is a primarily form of mesh refinement.

When studding a particular system, one ought to have a quite good idea of all the inputs that are under analysis. The relevant physical characteristics such as material properties, constrains, geometries and loads should be closer to the real as possible, since these will have a direct interference on the accuracy of results. When all of that data is correctly gathered, it is recommended to start the FEA study with a more course preliminary mesh, with broad element domains. Although its results may not be the most accurate, it still provides a verification of the system under study, much like debugging measure. If everything runs smoothly, only then a refinement of the mesh should occur. There are different approaches for refinement of the mesh once our system checks out.

Finer element domain size

Once the system under study is properly defined, by turning the mesh finer and finer at each iteration, each domain will be turned smaller as possible (fig. 13). This is an example of the most common mesh refinement used, due to its simplistic manner and due to its accuracy, however this may bring some inconvenience and constrains: the finer the mesh gets, more heavy the computation of results will get, and this may be a constraint if it gets to a point that the computer is simply not capable enough to handle such a heavy burden. Also, it will be very timely cost. So, although reducing the size of the elements is a good strategy, it should be made with care.

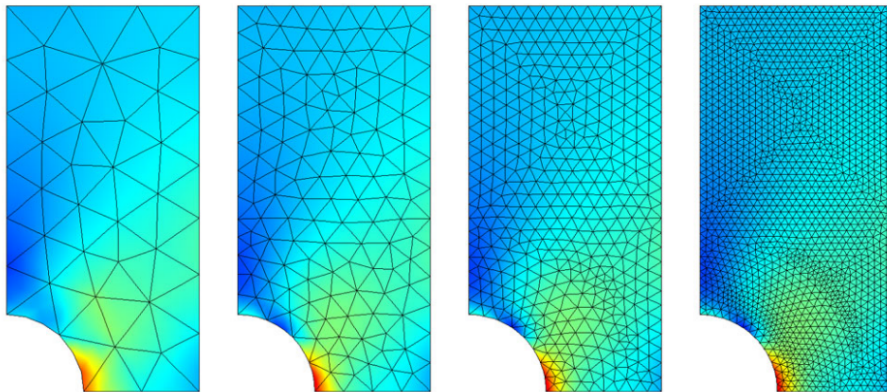


Figure 13: Example of a finer element refinement mesh [6]

Removing non relevant parts from system

Trying to solve an entire system as a whole may be difficult and expensive in terms of computing resources. Once analyzing a system, we should consider if all the details and elements are needed

to achieve the needed solution, or can these features be simply removed from the equation. Trying to reduce the complexity of the system without jeopardizing the outcome of the analysis by just removing sections of the elements without any direct influence on the process is a simple and effective measure.

On this analysis of the riveting, this refinement was a strategy used for the terminal. As depicted above on figure 7, only the top part of the terminal where the riveting occurs was used, being the rest of this component removed from the CAD prior to its analysis.

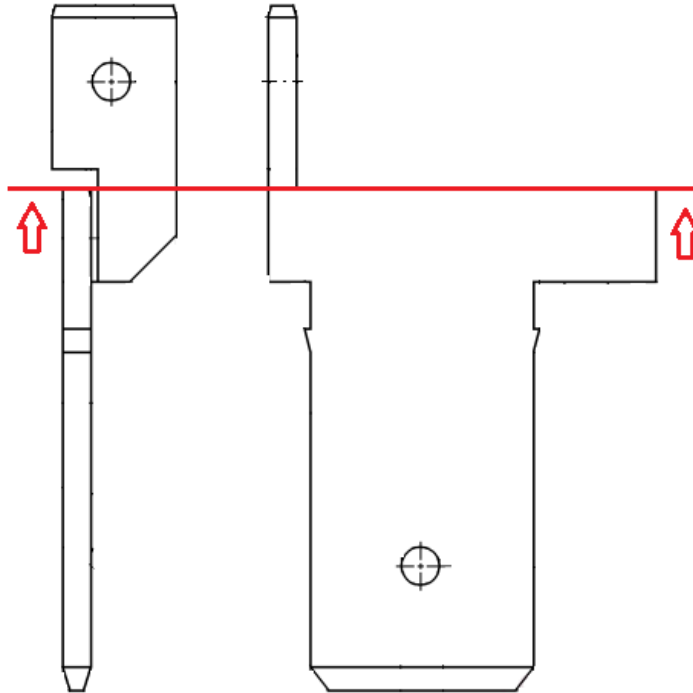


Figure 14: Section of the terminal removed from the simulation

Increasing element order

Increasing the element order (fig. 15) can be helpful in achieving a better result and has the advantage that no remeshing is needed, therefore there isn't any additional waste of time on that process which may sometimes be quite slow, especially when dealing with more complex geometries. With this particular strategy, basically we're using the same mesh, however, only the elements order is rearranged. Nonetheless this technique has a downside, which is that this will require much more computing capabilities, since it will cause our simulation to become heavier.

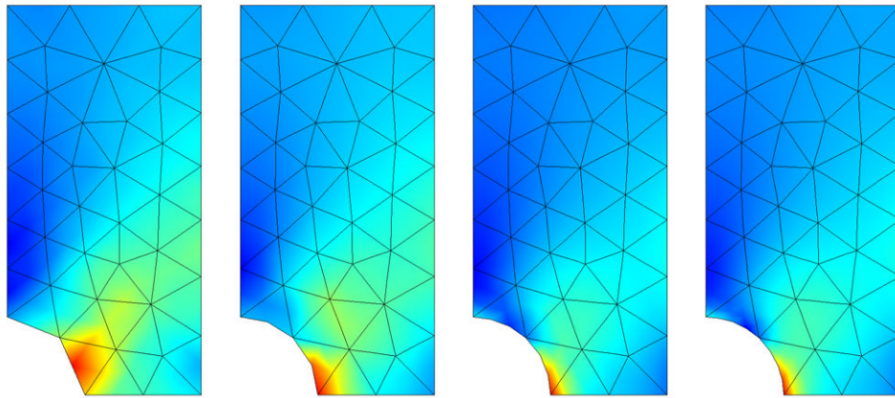


Figure 15: Example of increasing element order technique [6]

Local mesh refinement

With this technique of local mesh refinement (fig. 16), as the name suggests it, we'll be dedicated to refine the mesh on one particular area, where the results have the utmost importance. This strategy differs from the outstanding techniques because in this one, the error will only be evaluated for a specific subset of our model. Thus, with this technique we'll become able to remesh the whole model with a special consideration for a specific area of an element, with the goal to reduce the area on that region, hence being able to have a finer mesh and therefore more accurate results for that area than we would have with the other mesh refinement strategies.

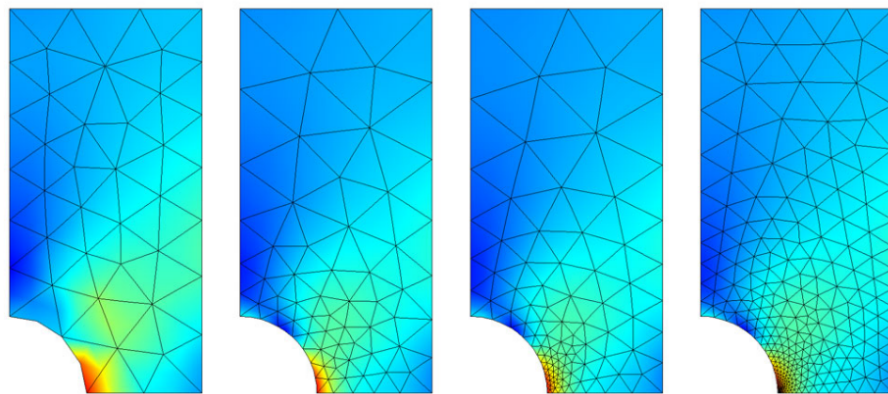


Figure 16: Example of local mesh refinement technique [6]

6.2 Simulation results

In figure 17 is depicted the results obtained from the simulation on the various stages of the riveting process, in particular the idle moment, the first moment when the punch starts deforming the rivet and the final moment, where the final displacement of the punch is reached, conferring the rivet's final geometry.

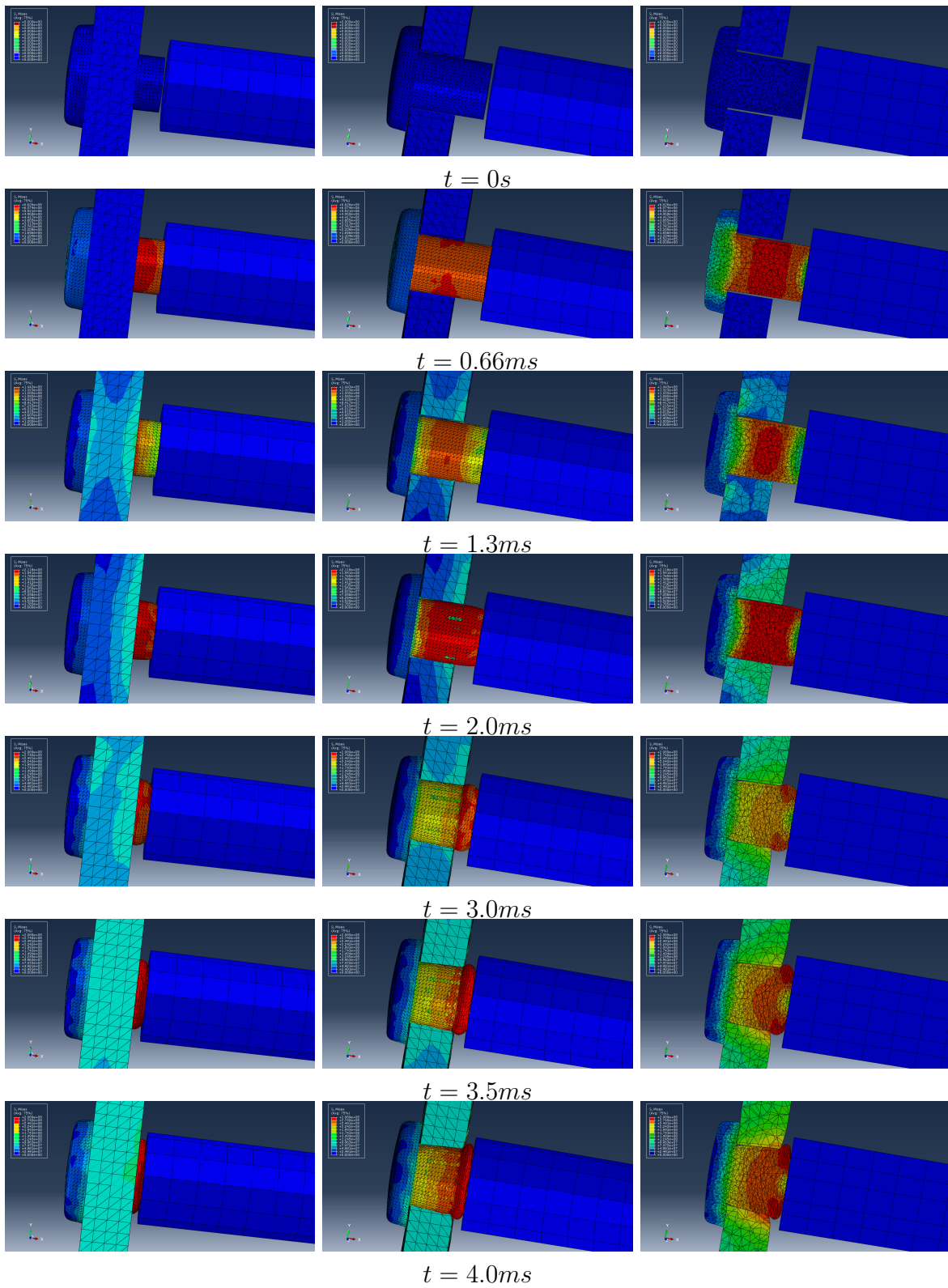


Figure 17: Riveting process: overall view, view without metal sheet frontal part and cross section view - von Mises equivalent tensile stress

From this simulation is also possible to withdraw the values for the reaction for each iteration of the punch displacement, therefore a graph depicting the Reaction versus Displacement was plotted and depicted at fig. 18.

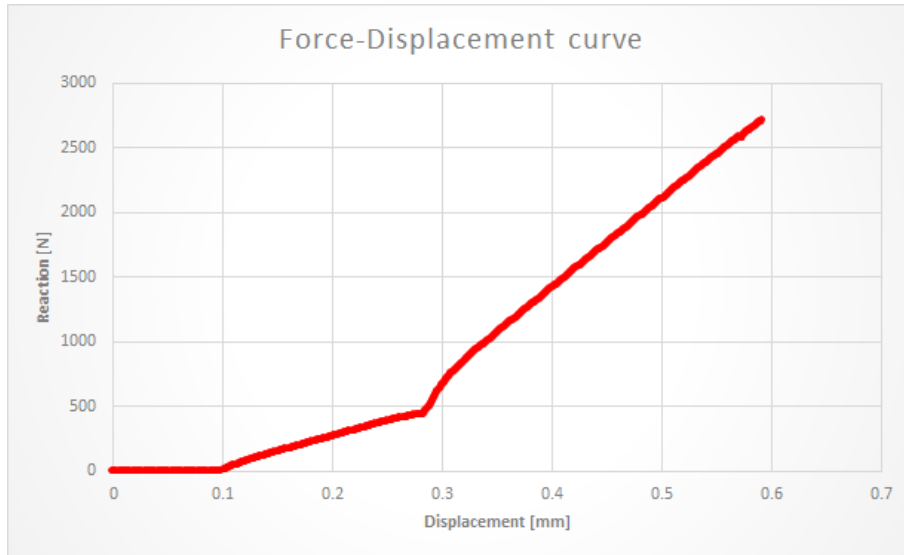


Figure 18: Simulation force/displacement graph

6.3 Analysis and comparison of results

Once the simulated characteristic curve for the expected behaviour is attained, we then proceed to comparing it to the data gathered from this very own machine. As previously stated on chapter 4, this particular machine is equipped with a load cell, displacement sensor and display from Kistler®), hence enabling a 100% control onto this riveting process, therefore, we'll compare the expected behaviour with this data gathered live from the machine from several different days, since there's always some slight differences on the admissible outcome of the process.

So, in order to determine if the simulation carried out is accurate, its results were directly compared to the results retrieved live from the riveting process.

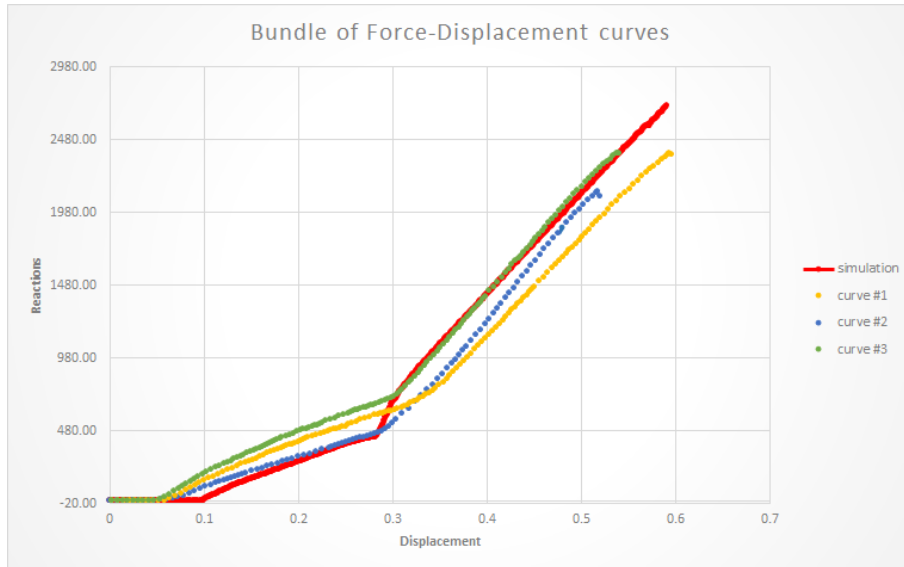


Figure 19: Comparison between rivet experimental and simulation behaviour

As it may be seen in fig. 19, the bundle of curves where the simulation is in are quite similar, either in terms of displacement and in terms of the total force, nonetheless, it is still possible to notice some differences between those. Even between the experimental force-displacement characteristic curves, and overlooking the simulated curve, we may see that there's some differences. These differences are due to the process normal variation, since each of these curves belong to parts produces in different days with different raw material batches, with the machine in different needs of maintenance and even with different operators, therefore is no wonder that is noticeable a slight difference between the expected (simulated) and the obtained (experimental), although the simulated (in red) and experimental curve #3 (in green) are fairly similar.

Moreover, there's also a common difference between the simulated and all the experimental, which is the fact that these last ones start to have an increasing of the force some tenth of the millimeter sooner than the simulation. This phenomenon is easily explained by the fact that the machine punch in order to move and to expose its tip and therefore to complete its full course, has to press a compression spring, thus promoting an earlier debut of a force, aspect which was not considered on the simulation, where the displacement measured is simply the punch movement.

With that said, the variation verified on the normal process behaviour (fig. 20), thus its standard variation, is typically called as the process sigma (σ). After the machine instrumentation, and retrieving of the curves, the purpose is to analyze this data and its sigma, and to define and implement control limits with the drive to establish not only a control on the final product but also to have a controlled process.

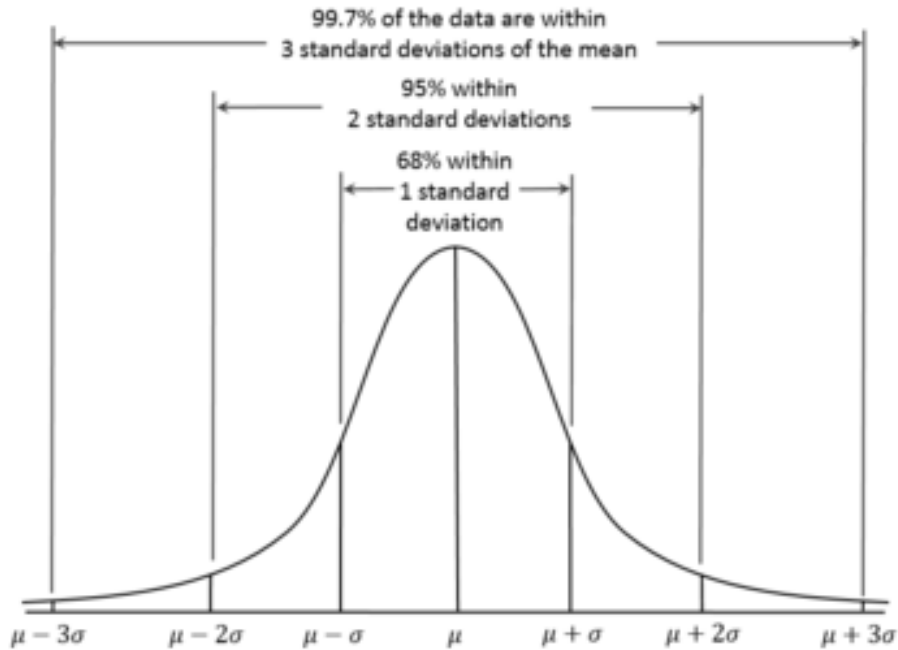


Figure 20: Gaussian distribution [23]

So, by comparing the bundle of curves where the simulated and the experimental results are figured in, we may clearly noticed that these are fairly similar. Furthermore, it is also relevant to compare the aspect of the outcome between the simulation and experimental results from this riveting. In order to do so, we've compared intact riveted parts as well as crossed section analysis of the product from the experimental and put it side by side with full and cross sectional view from the experimental data, as it may be seen on figure 21.

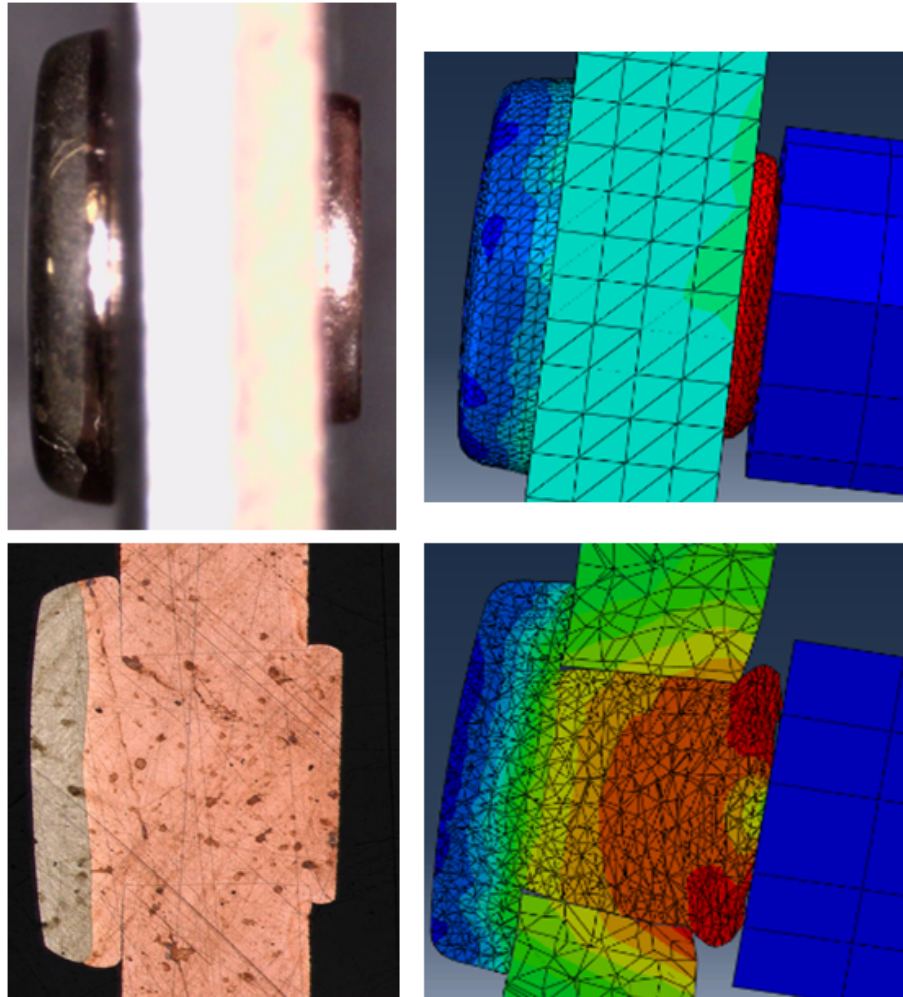


Figure 21: Experimental Vs Simulated riveting (von Mises)

Hence, by appraising either the Force vs Displacement characteristic bundle of curves and the aspect of the final product we may dare to state that the simulation was successful and is representative of the mechanism that occurs throughout this process.

7 Electrostatics and full temperature coupling

After achieving a proper simulation of this riveting process, it becomes relevant to analyse the electric current path throughout this model. This analysis has the purpose to observe and detect any eventual abnormalities with the current flow, and to assure that this part is indeed suitable to act as a contact able to conduct an electrical load. This time, resorting to *SIMPLAS* software, we'll inject a nominal load of 70 A and we will simulate the thermo-electrostatic coupling of these two parts, based on the model obtained from the previous ABAQUS simulation.

We consider a volume domain V and its boundary S , along with the normal \mathbf{n} to the outer surface S . At this surface, a current density (current per unit area) \mathbf{J} is introduced. In the volume V , we identify ρ_c as the volumetric current source (current *source* per unit volume). For steady-state direct current, Maxwell's equation of conservation of charge [2] is materialized by the following balance between surface and volume quantities:

$$\int_S \mathbf{J} \cdot \mathbf{n} dS = \int_V \rho_c dV \quad (10)$$

Ohm's relation between current density \mathbf{J} and the electric field \mathbf{E} is made possible by the introduction of the electric conductivity matrix \mathbf{C} . A linear relation between the current density and the electric field is used, which is introduced as:

$$\mathbf{J} = \mathbf{C} \cdot \mathbf{E} \quad (11)$$

The relation between the electric field \mathbf{E} and the electric potential φ is classical and reads:

$$\mathbf{E} = -\frac{\partial \varphi}{\partial \mathbf{X}} \equiv -\partial_{\mathbf{X}} \varphi \quad (12)$$

We note that, in (11), the electric conductivity matrix is dependent, in general, on the temperature:

$$\mathbf{C} \equiv \mathbf{C}(T) \quad (13)$$

We can now obtain a weak form of (10) by the introduction of a test function $\hat{\varphi}$, which is multiplied in both sides of the integrands in (10). After integration by parts of the result, the weak form is finally obtained:

$$\int_V \partial_{\mathbf{X}} \hat{\varphi} \cdot \mathbf{C} \cdot \partial_{\mathbf{X}} \varphi dV = \int_{S_J} \hat{\varphi} J dS_J + \int_V \hat{\varphi} \rho_c dV \quad (14)$$

where J is the imposed (or *injected*) current on surface. We here partition the surface S in two, one part S_φ where φ is known and one part S_J where J is known. Equation (14) is of course elliptic as long as \mathbf{C} is positive-definite. In the context of Joule's effect, the volumetric heat source is given by:

$$\dot{Q} = \partial_{\mathbf{X}} \varphi \cdot \mathbf{C}(T) \cdot \partial_{\mathbf{X}} \varphi \quad (15)$$

Table 7: Copper thermo-electric properties

Quantity	Description	Units
\mathbf{C}	Conductivity matrix	Sm^{-1}
\mathbf{E}	Electric field	Vm^{-1}
J	Injected current at a surface	Am^{-2}
\mathbf{J}	Current density	Am^{-2}
\mathbf{n}	Unit normal	–
\dot{Q}	Volumetric heat source	Wm^{-3}
\dot{q}	Surface heat source	Wm^{-2}
\mathbf{R}	Resistivity matrix	Ωm
S	Surface	m^2 (measure)
T	Temperature	K
V	Volume	m^3 (measure)
\mathbf{X}	Position	m
ρ_c	Volumetric current source	Am^{-3}
φ	Electric potential	V
c	Specific heat	$\text{JKg}^{-1}\text{K}^{-1}$
R_{ref}	Reference resistivity	Ωm
T_{ref}	Reference temperature	C
α	Heat sensitivity	C^{-1}
λ	Heat conductivity	$\text{Wm}^{-1}\text{K}^{-1}$
ρ	Mass density	Kgm^{-3}
I	Current	A

which is the volumetric heat source in Fourier's equation. The weak form of Fourier heat's equation is given by:

$$\int_V \rho c \hat{T} \dot{T} dV + \int_V \lambda \partial_{\mathbf{X}} \hat{T} \cdot \partial_{\mathbf{X}} T dV = \int_V \hat{T} \dot{Q} dV + \int_{S_q} \hat{T} \dot{q} dS \quad (16)$$

which is a parabolic partial differential equation. We here partition the surface S in two sets, one set S_T with known T and set part S_q with known \dot{q} . Solutions of equations (14) and (16) have $\mathbf{X} \in V$ as represented in Figure 22.

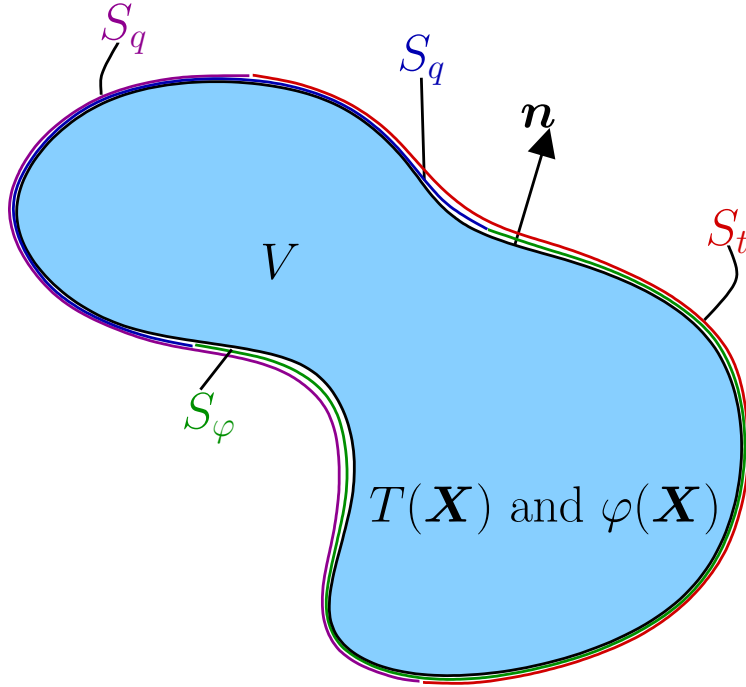


Figure 22: Domain for \mathbf{X} , eqs. (14, 16) and partitioning of the boundary.

For most metals, the resistivity matrix ($\mathbf{R} = \mathbf{C}^{-1}$) is a function of the temperature:

$$\mathbf{R} = \mathbf{C}^{-1} = R_{\text{ref}} [1 + \alpha (T - T_{\text{ref}})] \mathbf{I} \quad (17)$$

We present the relevant properties for *copper* in Table 8. Properties R_{ref} , α and T_{ref} are taken from R.A. Matula [1]. The considered boundary conditions are shown in Figure 23 over the deformed mesh from elastoplastic analysis. Results for the temperature and electric potential are exhibited in Figure 24.

Table 8: Copper thermo-electric properties

Property	Value	Units
ρ	8960	Kg m^{-3}
c	390	$\text{J Kg}^{-1}\text{K}^{-1}$
λ	385	$\text{W m}^{-1}\text{K}^{-1}$
R_{ref}	1.68×10^{-8}	Ωm
α	0.0039	C^{-1}
T_{ref}	20	C
I	70	A

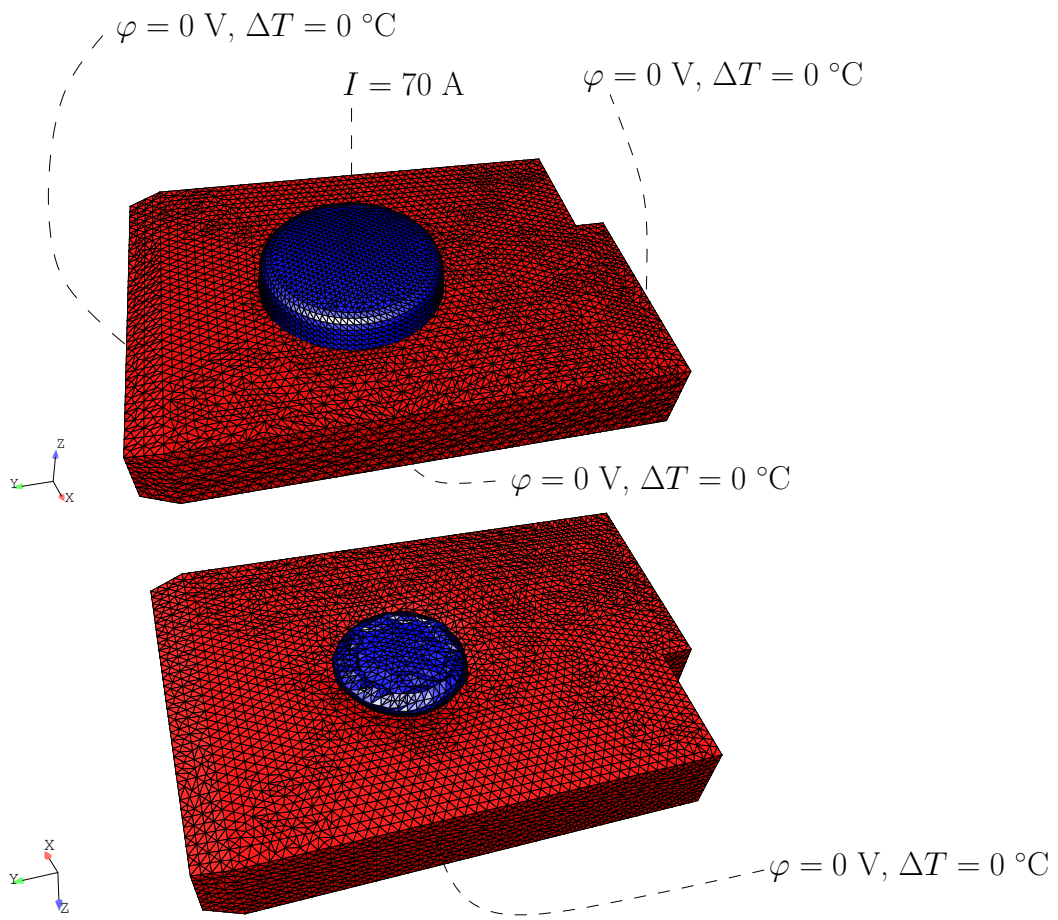


Figure 23: Simulation of rivet heat and current. Boundary conditions over the deformed mesh from elastoplastic analysis.

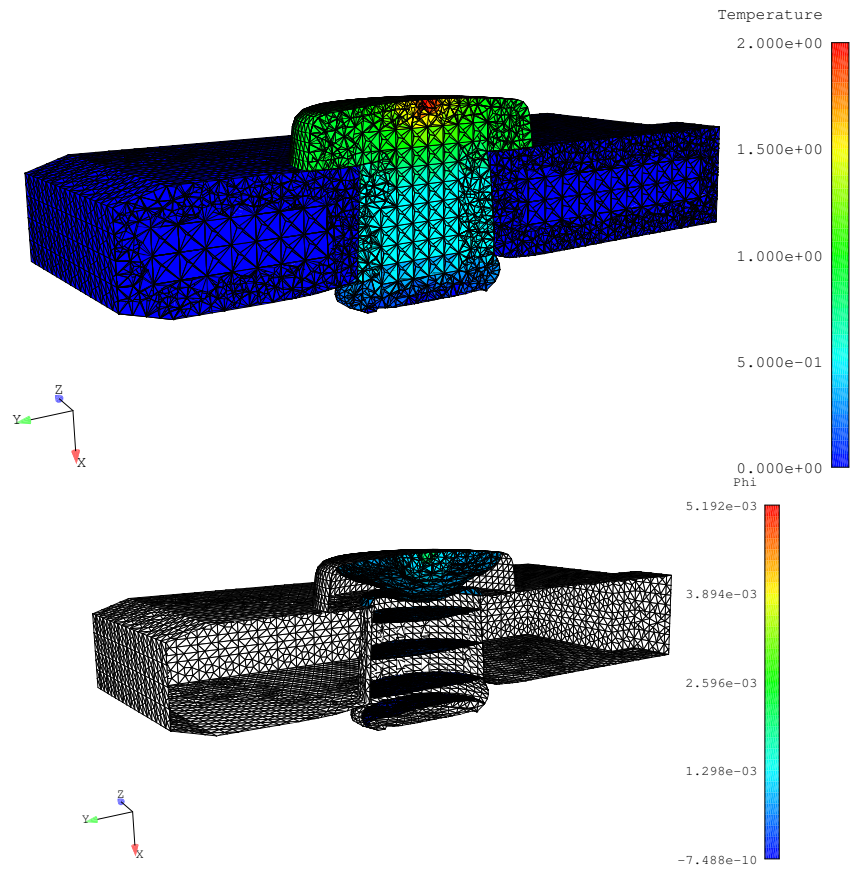


Figure 24: Simulation of rivet heat and current. Temperature and electric potential contour plots.

8 Optimization

As approached on the previous chapters, it did become possible to simulate the behaviour of this particular riveting process with some relative precision, as demonstrated when comparing the theoretical behaviour curve obtained from the CAE software simulations with the behaviour curves obtained from the real process, hence allowing the possibility for one to know and understand before any instrumentation whatsoever, what's going on with its riveting and what the critical stages of this process that are convenient to have under control.

However, although this riveting is now properly assessed, some other pertinent inquiries arise, such as, “how much deformation does the rivet shank really need for a solid riveting is attained?”, “is it really necessary to press that much the rivet shank or should we press it even more?”, or even more relevant for the sake of the machine and its components, “how much does the parameterization of this process affects the punch lifetime?”.

8.1 Optimal riveting

This riveting procedure, as summarized before, has two main goals which are rather important to meet, and that without any of those requirements being fulfilled, will most certainly result in a failure of the main product in which these parts are supposed to be assembled, in this particular case, a relay. These important and yet simple characteristics to be met are:

- Proper electrical contact between rivet and metal sheet;
- Sturdy mechanical connection (solidarity) between rivet and metal sheet (terminal);

To assure both requirements, we need for the rivet shank to fill in the terminal hole and get in contact with its internal walls, to have no gaps between rivet head and terminal, and to have the rivet shank overlapping the terminal after riveting, hence assuring that the electric current have a proper path to flow and that the rivet will not fall nor dislocate from its original place throughout the entire lifetime of the product.

In a way to analyze when these conditions are gathered, we're going to consider the results from the riveting simulation on every iteration, thus allowing to understand the moment where the ideal rivet deformation occurs.

As depicted below in figure 25, where U_2 represents the displacement (m) along the Y axis, we may notice that along the several iterations, the rivet shank start to barreling till it reach the metal sheet inner walls on both sides, in a way that this rivet-terminal gap is filled in as best as possible, thus achieving one of the premisses for this whole process.

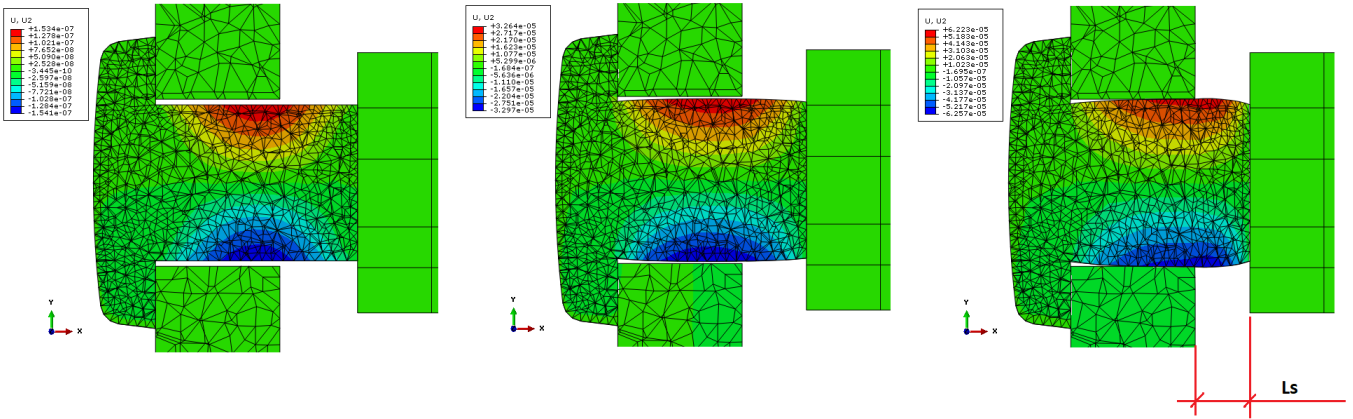


Figure 25: Rivet shank displacement at Y

By looking at the rivet shank displacement along Y axis, we can notice that while barreling, it expands approximately 0.125 mm , which coincidentally is exactly the difference between rivet shank and terminal hole, therefore assuring that there is a decent contact between these two, thus securing a correct path for the electric current to flow. As far as this rivet-terminal gap filling condition is concerned, this situation is attained at the occasion when the overhanging rivet shank (length of the shank - L_s) measures 0.527 mm .

However, accomplishing the condition above is important but it's not everything, thought by just having the terminal hole filled, it does not assures that the rivet will stay thigh onto its place throughout the entire product lifetime. To do so, it is desirable for the part of the rivet shank that overhangs throughout the terminal hole, to also overlap it, in a way to lock the rivet in its position, which under normal circumstances will guarantee that this part won't fall from its place.

Yet again, the simulation results are going to be evaluated at each iteration, in order to realize the moment when the rivet is properly locked and secured into its place. To do so, we're going to look at the plastic strain at Y axis, so a clear image of the rivet shank overlapping the terminal hole is attained.

So, by looking at figure 26, we may notice that this last mandatory characteristic of having a sturdy mechanical connection is going to be achieved when the plastic deformation of the rivet shank start to occur especially along the Y axis, hence allowing us to realize that the rivet will be locked onto the terminal, approximately when $L_s = 0.410\text{mm}$, meaning that for a terminal hole of $\phi = 1.625\text{mm}$ and for a rivet shank under this material conditions, with a $length = 0.750\text{mm}$ and $\phi = 1.5\text{mm}$, only roughly 45% of the rivet shank that overhangs from the terminal is needed to be deformed in order to have it rightfully notched onto its position. So, being aware of that the current riveting process produces rivets shanks with $L_{s_{process}} \approx 0.30\text{mm}$, and according with the previous simulation results, it seems that we're deforming these rivets 0.11mm further than what seems necessary.

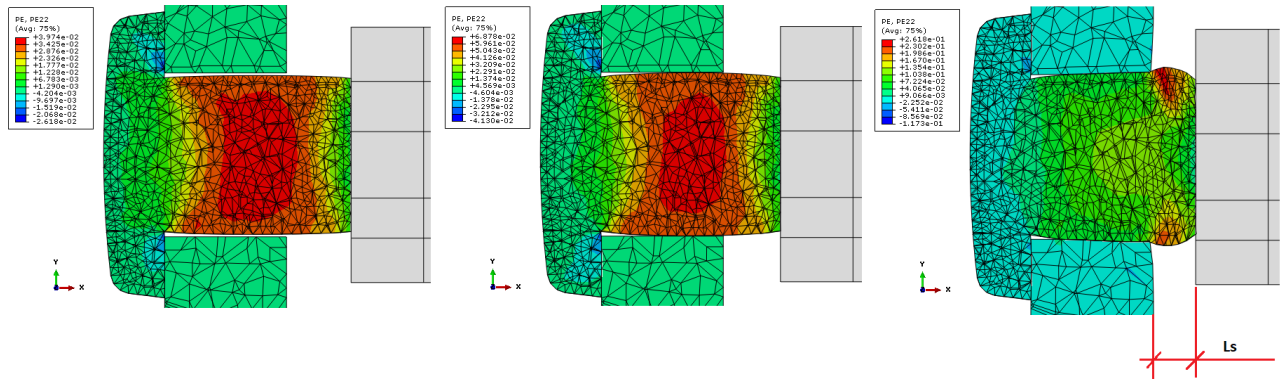


Figure 26: Rivet plastic strain at Y

8.2 Punch deterioration

So, has it was examined, although it seems that we may have been notching this rivet slightly too much, it has no side effects on the riveting itself. As long as the conditions for the rivet integrity are met and as long as this over notching does not deform the terminals nor produces cracks on the rivet or any other type of imperfections, as far as the riveting process is concerned, it seems to be alright. However, on other hand, this unnecessary over notching may have some adverse results on the main machine elements involved on this production process, namely, punch and counter punch. As a way to analyze the effect of this notching parameters on the punch life time , we're going to assess the contact pressure, which is factual known as a major influence.

Contact pressure, as the name suggest it, is the ratio of the perpendicular load versus the contact area of a given surface. It is a rather important factor to consider especially on tools which are under friction, cyclic stress and high mechanical loads, aspects which may result in wear and eventually fractures due to mechanical fatigue of the tool itself, therefore as mentioned, decreasing the tool normal life time. Thus for this reason, the material of such elements/tools to use, in order to withstand such a heavy-duty enviroment must have at some degree a good resistance to wear and a high fracture toughness, therefore material such as HSS (High Speed Steel), which is our particular case, and other molybdenum based steels are favored to be used.

So, from the simulation results is possible to withdrawn the data from the contact pressure exerted into the punch surface, as well as the rivet shank displacement (fig.27), which will allow us to understand if and when this tool may be overloaded beyond what is recommended for such element to withstand.

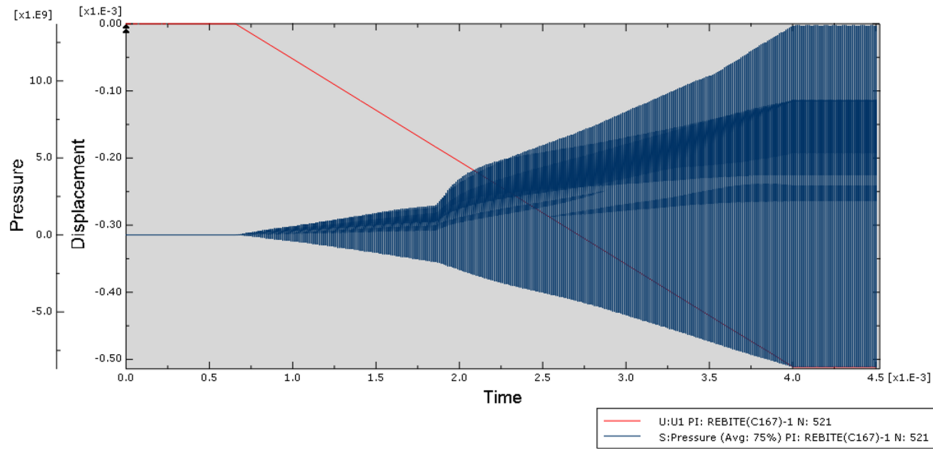


Figure 27: Pressure (GPa) and Displacement (m) versus Time (s)

Additionally, considering the work of N. Karunathilaka and others [20], we're going to set a threshold for the contact pressure for HSS at 2.25GPa. With this information and breaking down the data gathered from the the simulation for pressure and displacement, it's going to be possible to notice when in time this contact pressure is reached, and at what moment of the riveting is attained.

As depicted at fig.28, by crossing the pressure moving average from our data with the 2.25GPa threshold, we'll have that these two intercept at about 0.0039s.

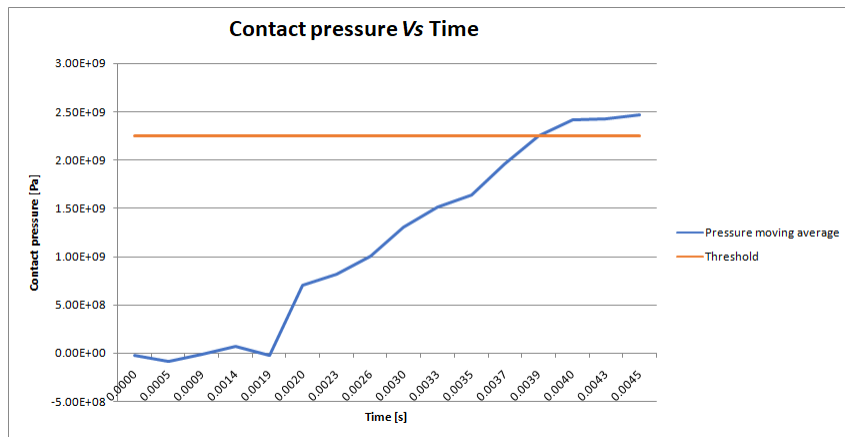


Figure 28: Contact pressure over time

Moreover, knowing that this threshold occurs at 0.0039s and resorting to fig.29, we can reach the conclusion that the riveting process, for the sake of the punch, should not deform this rivet over 0.495mm, thus leaving an ideal maximum for $L_s = 0.255mm$.

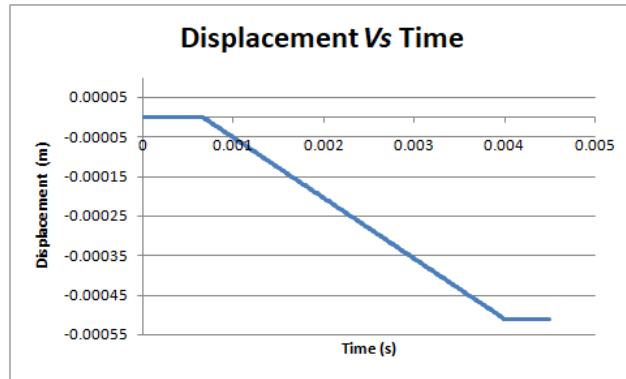


Figure 29: Rivet displacement over time

Hence, if we take a look into the riveting simulation moment which is depicted at fig. 30, where $L_s = 0.255mm$, we'll see that the riveting is far too much ahead of the two earlier situation discussed at point 8.1. as it clearly locked into position, as at this moment, practically no plastic strain is occurring any longer along at Y axis. Thus, we may state that concerning the wear of the punch, this process does not seems to present any threat as long as the riveting is not exaggerated, therefore, according to the simulation, ideally this riveting should be at $L_s = [0.255; 0.300] mm$.

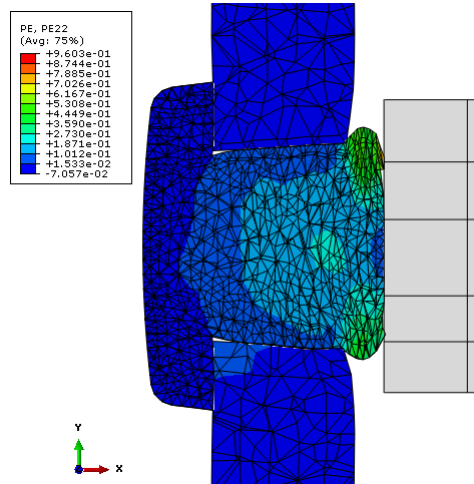


Figure 30: Riveting at contact pressure advisable limit

9 Conclusion

Globally the simulation was carried out successfully, as it may be seen when comparing the actual Force-Displacement curve obtained from the equipment installed at this very machine which the curve plotted from the results obtained from Abaqus simulation. This also means that the boundary conditions were properly defined, although no counter-punch was set into this simulation, and instead, it was considered that the rivet head is constrained along X, Y and Z. Furthermore, these positive results also mean that the main elements involved in this riveting process, i.e., rivet, terminal and punch were accurately characterized in terms of its material's properties, especially the rivet, which due to the lack of information regarding this peculiar kind of material, its hardening curve had to be characterized by performing experimental laboratorial testing. Although if we thoroughly look at the bundle of curves containing simulated and experimental Force-Displacement curves we may observe some differences, this disparity doesn't seem to be enough to raise any concerns regarding the accuracy of our simulation, since the simulated was considering an ideal situation, with no imperfections, inputs variations, machine's mechanical looseness and compression spring from the punch holder.

Moreover, one simple and yet important factor for the accuracy of the results was also the meshing. On the most important component, which was the rivet, element to be mainly deformed, it was used a rather fine mesh, so the results attained would rather be more rigorous. On other hand, on elements like the punch, where isn't expected any kind of elastic nor plastic deformation, it was used a more coarse mesh. So, although theoretically it wouldn't make any difference using the same mesh refinement from all the elements, this would severely impact the time needed for the processing of these results, hence the reason why there's different meshes.

An electrostatics and temperature coupling analysis was also performed by resorting to Simplas finite element software [22] upon the deformed mesh obtained from the simulation, with the intention to observe any possible abnormality with the current path or any unusual overheating that might be occurring when injecting a nominal current of 70A at the center of the riveting, yet nothing atypical was detected.

Finally, an optimization analysis was held considering the inspection of the several iterations derived from the Abaqus simulation results, with the goal to reach an optimal riveting point where the rivet would be securely tight into the terminal and also the wear of the tool that performs this task to be the minimum as possible. As it was seen, as long as the riveting is not exaggerated, there shouldn't be any problem whatsoever regarding the punch deterioration, as it was seen that the advisable contact pressure threshold is only reached almost at the very end of this process, thus, it is favored to have $L_s = [0.255; 0.300] \text{ mm}$, where this rivet is thigh, and the punch deterioration is virtually non-existence.

10 Acknowledgements

I would like to thank INEGI institute for performing the laboratory tests in a way to characterize the hardening curve of this particular rivet, so we could have a very much needed knowledge about its plastic behaviour, thus greatly contributing for having a simulation closer to reality.

Also, I would like to thank TE Connectivity for allowing me to write this work about one of their processes, which prove to be a quite interesting subject for study and also for any possible further developments.

Last but not least, I would like to express my most sincere gratitude to Prof. Pedro Areias and Prof. Manuel Pereira dos Santos, which were always available for me and so thoroughly guided me through this work. Without their valuable cooperation this work would not be done.

References

- [1] R.A. Matula. Electric resistivity of copper, gold, palladium and silver. *J. Phys. Chem. Ref. Data*, 8(4):11471298, 1979
- [2] P.A. Tipler and G. Mosca. *Physics for Scientists and Engineers*. W.H. Freeman and Company, New York, NY 10010, sixth edition, 2008
- [3] Carreker, R.P., Hibbard, W.R. Tensile deformation of high-purity copper as a function of temperature, strain rate, and grain size. *Acta Metallurgica*, 654–663 (1953).
- [4] Two-dimensional CFD simulation for visualization of flapping wing ornithopter studies - Scientific Figure on ResearchGate. Available from: https://www.researchgate.net/figure/Figure-5-Schematic-of-the-a-Structured-mesh-and-b-Unstructured-mesh_fig2_284732956 [accessed 29 Jun, 2020]
- [5] Jung, Yong Su & Govindarajan, Bharath & Baeder, James. (2016). A Hamiltonian-Strand Approach for Aerodynamic Flows Using Overset and Hybrid Meshes.
- [6] Finite Element Mesh Refinement - Multiphysics cyclopedia. Available from: <https://www.comsol.pt/multiphysics/mesh-refinement> [accessed 21 Feb, 2020]
- [7] What is a Mesh? - Simscale documentation. Available from: <https://www.simscale.com/docs/simwiki/preprocessing/what-is-a-mesh/> [accessed 21Feb, 2020]
- [8] H.D. Chandler, Work hardening characteristics of copper from constant strain rate and stress relaxation testing, *Materials Science and Engineering: A*, Volume 506, Issues 1–2, 2009, Pages 130-134, ISSN 0921-5093
- [9] Blanchot, V. & Daidié, Alain. (2006). Riveted assembly modelling: Study and numerical characterisation of a riveting process. *Journal of Materials Processing Technology*. 180. 201-209. 10.1016/j.jmatprotec.2006.06.005.
- [10] Chen, Nanjiang & Ducloux, Richard & Pecquet, Christel & Malrieu, Julien & Thonnerieux, Maxime & Wan, Min & Chenot, J.L.. (2011). Numerical and experimental studies of the riveting process. *International Journal of Material Forming*. 4. 45-54. 10.1007/s12289-010-0987-6.
- [11] Blanchot, V. & Daidié, Alain. (2006). Riveted assembly modelling: Study and numerical characterisation of a riveting process. *Journal of Materials Processing Technology*. 180. 201-209. 10.1016/j.jmatprotec.2006.06.005.
- [12] Zhang, Kaifu & Cheng, Hui & Li, Yuan. (2011). Riveting Process Modeling and Simulating for Deformation Analysis of Aircraft's Thin-walled Sheet-metal Parts. *Chinese Journal of Aeronautics - CHIN J AERONAUT*. 24. 369-377. 10.1016/S1000-9361(11)60044-7.

- [13] Yu, Haidong & Zheng, Bin & Xu, Xun & Lai, Xinmin. (2019). Residual stress and fatigue behavior of riveted lap joints with various riveting sequences, rivet patterns, and pitches. Proceedings of the Institution of Mechanical Engineers, Part B: Journal of Engineering Manufacture. 095440541983448. 10.1177/0954405419834481.
- [14] Shrot, Aviral & Baeker, Martin. (2011). How To Identify Johnson-Cook Parameters From Machining Simulations. AIP Conference Proceedings. 1353. 10.1063/1.3589487.
- [15] Basan, R. & Marohnic, Tea. Constitutive Modeling and Material Behavior, University of Rijeka, Rijeka, 2016
- [16] A.V. Sobolev, M.V. Radchenko, Use of Johnson–Cook plasticity model for numerical simulations of the SNF shipping cask drop tests, Nuclear Energy and Technology, Volume 2, Issue 4, 2016, Pages 272-276, ISSN 2452-3038
- [17] Damage initiation for ductile metals. Available from: <https://abaqus-docs.mit.edu/2017/English/SIMACAEMATRefMap/simamat-c-damageinitductile.htm> [accessed 30 Mar, 2020]
- [18] Johnson-Cook Plasticity. Available from: <http://bobcat.nus.edu.sg:2080/English/SIMACAEMATRefMap/simamat-c-johnsoncook.htm> [accessed 30 Mar, 2020]
- [19] Specific Heat of Solids. Available from: https://www.engineeringtoolbox.com/specific-heat-solids-d_154.html [accessed 4 Jan, 2020]
- [20] Karunathilaka, Nuwan & Tada, Naoya & Uemori, Takeshi & Hanamitsu, Ryota & Kawano, Masahiro. (2018). Effect of contact pressure applied on tool surface during cold forging on fatigue life of tool steel. Procedia Manufacturing. 15. 488-495. 10.1016/j.promfg.2018.07.258.
- [21] Unstructured Mesh Layers - Github.com. Available from: <https://github.com/lutraconsulting/qgis-crayfish-plugin/issues/335> [accessed 21Feb2020]
- [22] Areias, Pedro. *SIMPLAS, Nonlinear, nonsmooth finite element software*. Retrieved from <http://www.simplassoftware.com/index.html>
- [23] Gaussian Distribution - Lean six sigma definition. Available for: <https://www.leansixsigmadefinition.com/glossary/gaussian-distribution/> [accessed 22Feb2020]